Hamlyn Symposium on Medical Robotics 2022
10.31256/HSMR2022.65

Modeling Telescoping Tendon-actuated Continuum Robots

Yash Chitalia, Abdulhamit Donder, and Pierre E. Dupont
Department of Cardiovascular Surgery, Boston Children's Hospital,
Harvard Medical School, Boston

INTRODUCTION

Tendon actuation is the most common method for producing flexure in continuum medical devices. Examples include catheters, ureteroscopes, bronchoscopes and colonoscopes. These devices are comprised of an elongated tube with a short steerable tip portion and a long passively flexible proximal portion. The shape of the proximal portion conforms to the shape of the body lumen as it is advanced into the body while the tendon-actuated tip portion provides for tip positioning and steering.

While many of these devices are comprised of a single elongated tube, there are important clinical examples for which a single steerable tip section is insufficient and the increased steerability provided by additional telescoping steerable sections is needed (Fig. 1). For example, the delivery systems used for heart valve repair and replacement employ 2-3 tendon-actuated telescoping sections [1]. Additional examples include Hansen Medical's robotic electrophysiology catheter [2] and Auris Health's robotic endoscope for peripheral lung biopsies [3] each of which possess two telescoping steerable sections.

Fig. 1. Example tendon-actuated catheter comprised of two telescoping tubes.

While a variety of models mapping tendon actuation to robot shape have been developed, they are all limited to consideration of a single tube [4-6]. They cannot accurately predict the shape of multi-tube robots because they do not model the twisting that occurs between the tubes. The contribution of this paper is to produce a model that includes tube twisting and to illustrate it experimentally using the system of Fig. 1.

MECHANICS-BASED MODEL

Each tube is modeled as a Cosserat rod and tendons are modeled as Cosserat strings similar to [6]. The rod model expresses static equilibrium using differential equations for bending moment, $m \in \mathbb{R}^3$, and shear force, $n \in \mathbb{R}^3$, as functions of arc length, s. Kinematic inputs are given as tendon tension forces, *f*. Each tendon generates distributed forces along the length of the rod as well as concentrated forces and moments at their distal ends where they attach to the rod. Tendon equilibrium is described by a differential equation in shear force. Assuming no tendon friction, the tendon tension is constant along its length and shear force is tangent to the tendon.

Using constitutive laws relating bending moment and shear force to curvature and shear strain, respectively, Rucker and Webster show that these models result in a set of decoupled linear differential equations in curvature and shear strain [6]. To extend this model to multiple telescoping tubes, additional constraints and derivational techniques must be applied to arrive at a comparable set of linear differential equations.

Owing to the length of the derivation, only a summary of the approach and model are presented. For a set of telescoping tubes, each with its own tendons, the nominal set of state variables to be integrated for tube *i* is comprised of curvature, $u_i \in \mathbb{R}^3$, and shear strain, $v_i \in \mathbb{R}^3$. In the overlapping portions, however, the tubes conform to the same (body-frame) centerline, $p^b \in \mathbb{R}^3$. Using body-frame coordinates with the z axis directed tangentially, this constrains the x and y (bending) components of curvature to be equal for all overlapping tubes. Similarly, the cross-sectional (x and y) shear strain components must be equal in the overlapping portion.

Imposing these constraints reduces the number of independent state variable for q fully overlapping tubes from $6q$ (3 curvature components and 3 shear strain components for each tube) to $6 + 2(q-1)$. Here, the first 6 state variables are the curvature and strain components of the first tube (u_1 and v_1) while the additional state variables correspond to the z components of curvature and shear strain for tubes 2, ⋯,q.

Defining the torsional twist between tubes as $\alpha_i(s) = \theta_i(s) - \theta_1(s)$, in the body frame of tube 1, we have $\dot{\alpha}_i(s) = u_{i,z}(s) - u_{1,z}(s)$ where $\dot{\alpha}(s) = d\alpha(s)/ds$. For all functions of arc length, such as $\alpha(s)$, the *s* term is dropped in the remainder of this paper. The relationship between overlapping tube curvatures is given by

$$u_i = R_z^T(\alpha_i)u_1 + \dot{\alpha}_i e_3 \quad (1)$$

Here, $R_z(\alpha)$ is rotation matrix about the z-axis. Differentiation with respect to arc length,

$$\dot{u}_i = R_z^T(\alpha_i)u_1 + \dot{\alpha}_i[e_3]^T R_z^T(\alpha_i)u_1 + \ddot{\alpha}_i e_3 \quad (2)$$

Similarly, the constraint on shear deformation of the overlapping tube cross sections is given by

$$v_i|_{x,y} = R_z^T(\alpha_i)v_1|_{x,y} \quad (3)$$

Assuming that the untensioned tubes are straight, the constitutive model for each tube is given as

$$\begin{bmatrix} m_i \\ n_i \end{bmatrix} = \begin{bmatrix} K_{bt} & 0 \\ 0 & K_{se} \end{bmatrix} \begin{bmatrix} u_i \\ v_i - v_i^0 \end{bmatrix}, \quad v_i^0 = e_3, \quad (4)$$

We write the overall moment-curvature equilibrium equation by summing over all the overlapping tubes. For compactness, the expression below is written for two tubes and $[x]$ represents the skew symmetric form of $x \in \mathbb{R}^3$:

$$\dot{m}_1 + [u_1]m_1 + \left\{[u_1]R_z(\alpha) + \frac{dR_z(\alpha)}{d\alpha}\dot{\alpha}\right\}m_2 + R_z(\alpha)\dot{m}_2 + [v_1]n_1 + R_z(\alpha)[v_2]n_2 + \tau_1 + R_z(\alpha)\tau_2 = 0 \quad (5)$$

Here, τ_i represent the sum of moments applied to a tube by its tendons together with any external moments. Since, the tubes can be independently twisted, an additional equation is needed for the torsional moment of the second tube:

$$\dot{m}_{2,z} + ([u_2]m_2 + [v_2]n_2 + \tau_2)|_z = 0 \quad (6)$$

The shear strain equilibrium equation is obtained similarly. Here, summing for total shear strain equilibrium is done to cancel the distributed shear forces that each tube applies to the others. For two tubes, this yields:

$$\dot{n}_1 + [u_1]n_1 + \left\{[u_1]R_z(\alpha) + \frac{dR_z(\alpha)}{d\alpha}\dot{\alpha}\right\}n_2 + R_z(\alpha)\dot{n}_2 + f_1 + R_z(\alpha)f_2 = 0 \quad (7)$$

Distributed forces, f_i, are due to tendons and external loads. Since the tubes can stretch independently, an additional equation is needed for axial elongation of the second tube:

$$\dot{n}_{2,z} + ([u_2]n_2 + f_2)|_z = 0 \quad (8)$$

Using (1)-(4), the equilibrium equations can be written purely in terms of the state variables, namely, $x = [u_{1,x}, u_{1,y}, u_{1,z}, v_{1,x}, v_{1,y}, v_{1,z}, u_{2,z}, v_{2,z}]^T$. Tendon forces and moments can be formulated as in [6] resulting in a set of linear differential equations of the form

$$A\dot{x} = Bx + c \quad (9)$$

While expressions for A, B, c are too lengthy to include here, this equation can be integrated by inverting A at every time step. Kinematic inputs are the tendon tensions along with the relative tube translations and rotations at the base. Since tendon tensions produce point loads and moments at their distal ends [6], the equations are solved as a two-point boundary value problem.

EXPERIMENTAL MODEL COMPARISON

To demonstrate the twisting predicted by the multi-tube model, Fig. 2 provides a comparison with the single tube model for the catheter of Fig. 1. For comparison, the tips of the two tubes are aligned axially and the same overall cross section is used (two tubes: OD1 = 8mm, ID1 = 7.4mm; OD2 = 7.4mm, ID2 = 6.4mm versus one tube: OD = 8mm, ID = 6.4mm). Elastic moduli were experimentally estimated for the tubes and actual tendon radii were 3.9mm (outer tube) and 3.6mm (inner tube). The outer tube tendon is in the *x-z* plane and the inner tube tendon is in the *y-z* plane. Tendons were loaded individually and simultaneously to 14.7 N (1.5 kgf).

Fig. 2a shows that when a single tendon is loaded, both the single- and two-tube systems experience only bending and the two models overlap. When both tendons are loaded at 90° to each other, however, the two tubes twist along their length and more accurately predict the experimental tip position. Model-predicted twisting between the tendons that accounts for the difference in tip is plotted in Fig. 2b.

DISCUSSION

Initial experimental validation of the multi-tube model suggests its usefulness for real-time control of robotic catheters and endoscopes. Future work will investigate its use for controlling a robotic catheter for interventional cardiology.

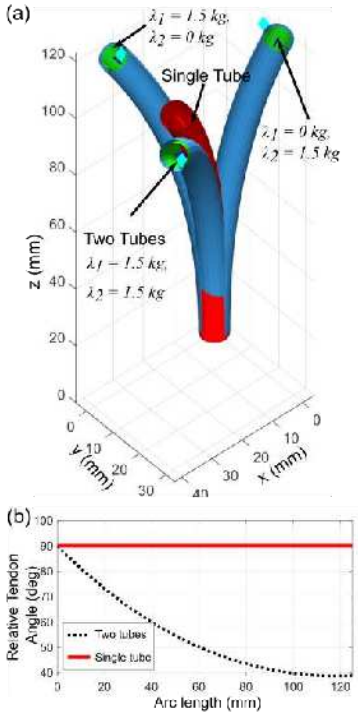

Fig. 2. Experimental comparison of single- and multi-tube models. (a) Catheter shape with tendons tensioned individually and simultaneously. (b) Relative tendon angle versus arc length.

REFERENCES

[1] M. Sherif, L. Paranskaya, S. Yuecel, S. Kische, O. Thiele, G. D'Ancona, A. Neuhausen-Abramkina, J. Ortak, H. Ince, and Oner, "Mitraclip step by step; how to simplify the procedure," Netherlands heart journal, vol. 25, no. 2, pp. 125–130, 2017.

[2] Al-Ahmad, J. D. Grossman, and P. J. Wang, "Early experience with a computerized robotically controlled catheter system," Journal of Interventional Cardiac Electrophysiology, vol. 12, no. 3, pp. 199–202, 2005.

[3] A. Agrawal, D. K. Hogarth, and S. Murgu, "Robotic bronchoscopy for pulmonary lesions: a review of existing technologies and clinical data," Journal of Thoracic Disease, vol. 12, no. 6, p. 3279, 2020.

[4] P. Rao, Q. Peyron, S. Lilge and J. Burgner-Kahrs, "How to Model Tendon-Driven Continuum Robots and Benchmark Modelling Performance," Frontiers in Robotics and AI. Vol. 7, 2021.

[5] F. Renda and C. Laschi, "A general mechanical model for tendon-driven continuum manipulators," Proc IEEE Int Conf Robotics and Autom, Saint Paul, MN, 2012.

[6] D. C. Rucker and R. J. Webster III, "Statics and Dynamics of Continuum Robots With General Tendon Routing and External Loading," IEEE Transactions on Robotics, vol. 27, pp. 1033–1044, 2011.